Analysis of the Published Calorimetric Evidence for Electrochemical Fusion of Deuterium in Palladium

GORDON M. MISKELLY, MICHAEL J. HEBEN, AMIT KUMAR, REGINALD M. PENNER, MICHAEL J. SAILOR, NATHAN S. LEWIS*

Estimates are given of the raw data that are the basis for the claims of excess power production by the electrochemical charging of palladium in deuterium oxide (D_2O). Calorimetric results are also presented that show no anomalous power production in either 0.1*M* LiOD/D_2O or 0.1*M* LiOH/H_2O (LiOH is lithium hydroxide). Several possible sources of error in open-system calorimetry are discussed that can confound interpretation of temperature changes in terms of anomalous power production.

THE PRIMARY OBSERVATION SUGgested as evidence for the cold fusion of deuterium (D) in palladium (Pd) is the production of excess power by the Pd, which was calculated to exceed the input power by factors of 4 to 8 under certain conditions (*1*). Numerous theories and experiments have been developed to explain these effects, but the raw data that reflect the actual magnitude and conditions of the observed excess power production were not presented in the original description of the work. The purpose of this report is to present these raw data and an analysis of the calculations used to obtain the large reported power production ratios. In addition, we describe some of our calorimetric measurements on the Pd/0.1*M* LiOD-D_2O/Pt cell. We also describe several subtle experimental details that must be considered to obtain accurate enthalpy values for an electrolysis reaction in an open calorimetric system.

When an aqueous solution is electrolyzed to liberate hydrogen and oxygen gas, the electrolysis power P_{app} ($=E_{app}\ I$) can be conveniently partitioned into two terms (Fig. 1):

$$P_{app} = E_{app}\ I = P_{cell} + P_{gas} \quad (1)$$

P_{gas} represents the power removed as a result of the evolution of H_2 (or D_2 in D_2O) and O_2 gases, and P_{cell} is the remaining power that is effective in heating the cell contents. An expression for P_{gas} ($= E_{gas}\ I$) is readily obtained from the known enthalpy of formation of water from its elements: $E_{gas} = -\Delta H_{form}/2F$ (F is Faraday's constant), which yields E_{gas} = 1.48 V for the reaction $H_2O \rightarrow H_2 + {}^1/_2O_2$ and E_{gas} = 1.54 V for the reaction $D_2O \rightarrow D_2 + {}^1/_2O_2$ (*2*). If the net faradaic efficiency of gas evolution, κ, is known, Eq. 1 for D_2O electrolysis then becomes

$$P_{app} = E_{app}\ I = [(E_{app} - \kappa\ 1.54\ V)\ I] + \kappa\ [(1.54\ V)\ I] \quad (2)$$

with the first term on the right equal to P_{cell} and the second term equal to P_{gas}. If no gas escapes from the cell (because of efficient recombination processes), then $\kappa = 0$, and Eq. 2 yields the expected $P_{app} = P_{cell}$, with all of the applied power resulting in heating of the cell contents. Alternatively, if the gases escape with unit efficiency, then $\kappa = 1$, and $P_{cell} = (E_{app} - 1.54\ V)\ I$. This latter condition results in the minimum heating of the cell for a given value of P_{app}.

In their analysis of the calorimetric data (*1*), Fleischmann, Pons, and Hawkins assumed $\kappa = 1$ and therefore defined the excess power, P_{ex}, as the difference between the measured heating power in the cell, P_{meas}, and the expected value of $P_{cell} = (E_{app} - 1.54\ V)\ I$. This definition, combined with reported values of the excess power (*1*) and the various formulas used to calculate "percent of breakeven values" (see below), has allowed us to recalculate the raw calorimetric data for the experiments of Fleischmann *et al.* (*1*), which are presented in Table 1 (*3*).

Several features of the data in Table 1 are worthy of discussion. First, in most cases, the calculated values of P_{ex} are rather small percentages of the total input powers. Accurate error bars for the determination of P_{app}, P_{gas} and P_{meas} must be obtained to assess the significance of the reported P_{ex} values. Second, recombination losses have been assumed to be negligible (that is, $\kappa = 1.0$) in calculating P_{cell} and P_{ex}; if substantial recombination occurred, P_{cell} would increase, and this would result in smaller, or possibly negligible, values of P_{ex}. Only in the last two measurements does P_{meas} ($= P_{ex} + P_{cell}$) exceed P_{app}; thus, only in these two cases could an adjustment in the value of κ not completely account for the observed data. The extent of recombination of H_2 and O_2 is a sensitive function of the cell geometry, electrode history, voltage, use of a separator, and so on (*4, 5*), and, although it may be unlikely that κ approaches zero for all the cells under study, a rigorous analysis of the calorimetric data requires that κ be reported in order to obtain reliable values for P_{cell} and P_{ex}. Possible solvent evaporation losses make mass balance determinations based on the rate of liquid D_2O loss (*1*) a questionable method for establishing the value of κ; a more reliable method would be collection of the gases followed by volumetric and compositional analysis during the calorimetric measurements.

It is also of interest to outline the procedures used by Fleischmann *et al.* (*1*) to calculate the percent of breakeven values from the raw data in Table 1. In all cases, P_{ex} was defined as $P_{ex} = P_{meas} - P_{cell}$, assuming $\kappa = 1.0$ [that is, $P_{cell} = (E_{app} - 1.54\ V)\ I$]. The first calculated breakeven percentage value [column a in table 2 of (*1*)] then represents $(100 \times P_{ex})/P_{cell}$; column b in table 2 of (*1*) represents $(100 \times P_{ex})/P_{app}$. In both cases, decreases in κ from the assumed value of 1.0 would reduce the calculated values. In calculating the raw data of Table 1 above, we have used the percent breakeven data in column a in table 2 of (*1*), and the formula $(100 \times P_{ex})/P_{cell}$ to calcu-

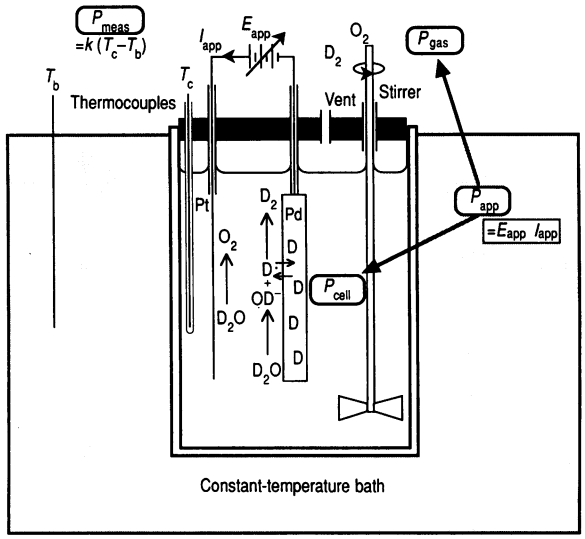

Fig. 1. Schematic of the calorimeter used in this work. The power applied through the electrolysis circuit $P_{app} = E_{app}\ I_{app}$ produces heating power delivered to the cell, P_{cell}, and to power contained in the evolved gases, P_{gas}. The temperature difference between the electrolysis cell and the constant-temperature bath is used to determine the heating power of the electrolysis circuit. Calibration and constancy of the heating coefficient, as well as the presence of thermal gradients, are key issues of concern for accurate power measurements in this system.

Division of Chemistry and Chemical Engineering, California Institute of Technology, Pasadena, CA 91125.

*To whom correspondence should be addressed.

late P_{cell} (and thus E_{app}); in some cases, using the reported data in column b in table 2 of (*1*), with the formula $(100 \times P_{ex})/P_{app}$ yields substantially different values for E_{app}, and these values have been indicated in parentheses in Table 1. In general, the P_{ex}/P_{app} ratios are rather modest and need to be considered carefully in view of possible changes in κ and errors in the determination of P_{meas}.

The actual applied voltages range from 2.8 to 10 V (Table 1), but column c in table 2 of (*1*) uses a voltage of 0.5 V to obtain $P_{app} = [(0.5\ V)\ I]$. The percent breakeven values in this column have been calculated as $(100 \times P_{ex})/[(0.5\ V)\ I]$. Of course, the assumption of $E = 0.5$ V yields much higher breakeven values than are calculated from the measured data, which display much larger E_{app} and P_{app} values.

The choice of a hypothetical value of 0.5 V involves the scenario where the electrolysis reaction does not evolve O_2 at the anode but rather oxidizes the D_2 generated at the cathode back to D_2O. In this case, only the voltages (overpotentials) required to overcome the electrode polarizations, solution resistance, and concentration gradients would contribute to the cell voltage, as the electrolysis voltage necessary to produce D_2 and O_2 from D_2O is eliminated. In principle, in optimal cell design, it is possible to envision a reduction in voltage to <1 V between two electrodes that have no other overvoltages. However, if the anode is to oxidize D_2, it must operate at potentials ≥0 V versus a reference Pt/D_2 electrode, while the instantaneous voltage measured after interruption of a current of 75 mA/cm² shows that the potential of a Pd/D electrode is 0.7 V more negative than that of a Pd/D reference charged to the α-β phase equilibrium (Fig. 2) and becomes even more negative when current is flowing through the circuit. Thus, the electrochemical potential required to maintain reasonable current densities through the charged Pd cathode is greater than the value of 0.5 V assumed by Fleischmann *et al.*, implying that the large hypothetical breakeven values calculated with the use of a value of 0.5 V are not experimentally attainable.

The measured quantity in the calorimetric experiments of Fleischmann *et al.* (*1*) is a cell power, not an enthalpy of reaction. Measurement of the power produced requires an accurate calibration of the rate of heat loss for all conditions of interest. To address these issues, we have performed several calorimetric experiments with both 0.1*M* $LiOD/D_2O$ and 0.1*M* $LiOH/H_2O$, using either a commercial isoperibolic calorimetry cell (Tronac, 50 cm³) in a 60-liter Tronac thermostatted bath (27.000° ± 0.005°C) or an air-jacketed vessel (30 cm³) in a 5-liter VWR bath (25.00° ± 0.04°C). Both cells were mechanically stirred and were calibrated throughout the experiments using the heat output from 100- to 340-ohm resistors. Current for the electrolysis and the calibration was supplied from Princeton Applied Research potentiostats (models 173, 273, or 362) or from Hewlett-Packard power supplies (model 6002A). Currents and voltages were measured with Fluke 75 or Keithley 177 multimeters, and temperatures were measured with the use of thermocouples, with the reference at the temperature of the surrounding bath. The counter electrodes were cylinders of platinum (Pt) foil or mesh (2 cm in diameter, 2 cm long), and the Pd electrodes were 2.0- to 2.4-cm lengths of rod of diameters 2.2, 2.1 to 2.3, or 3.9 mm, contacted either by spot welding to Pd or Pt wire, or by soldering to copper wire. All electrodes were completely immersed in the solutions at all times, and connections were insulated from the solution with glass tubing and epoxy resin. The electrolyzed water was typically replaced daily, during which time <5% of the solution was electrolyzed.

These calorimetric measurements led to the following observations. First, at all current densities (8 to 150 mA/cm²) and times (up to 170 hours) the measured heating powers in the $LiOD/D_2O$ cells were within 5% of the expected power calculated from Eq. 2 if we assume κ = 1.0, and the $LiOH/H_2O$ experiments gave results to within 6% of the predicted values. [Heat losses due to evaporation at the highest operating temperatures (49°C) are calculated to cause errors of less than 2% in the calculated heating power.] These measure-

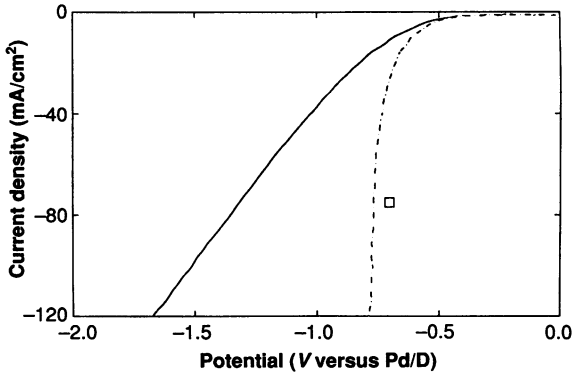

Fig. 2. Plot of the potentiostatic current-voltage characteristics for a charged Pd/D rod (0.254 mm in diameter, 2.7 cm long, charged for 14 hours at 64 mA/cm²) in 0.1*M* $LiOD/D_2O$. Potentials are with respect to a Pd wire charged to the α-β phase equilibrium; the reference wire was in a separate compartment filled with 0.1*M* $LiOD/D_2O$. This reference had a potential of −0.952 V with respect to a conventional saturated calomel electrode. (−) Directly measured data, scan rate = 10 mV/s; (— · — ·) data corrected for solution resistance; (□) potential measured 5 ms after interruption of a current density of 75 mA/cm².

Table 1. "Raw data" for electrolysis of D_2O at Pd. The data were calculated from table 1 and column a in table 2 of (*1*). The expected power produced in the cell was calculated from $(E - 1.54)\ I$, that is, on the assumption that there was no recombination of D_2 with O_2. The excess power produced in the cell is as quoted in table 1 of (*1*). The values in parentheses were calculated from column b in table 2 of (*1*). In all other cases, values calculated from column b agreed with those calculated from column a in table 2 of (*1*). The highest current entries for all three rods were measured on rods 1.25 cm long and rescaled to correspond to rods 10 cm long. In these calculations, we have ignored the areas at the end of the rods and have rounded the applied voltages to three significant figures while attempting to preserve the significance of the excess power data quoted in (*1*).

Applied current, *I* (mA)	Applied voltage, *E* (V)	Input power, $P_{app} = E\ I$ (W)	Power produced in cell, P_{meas} (W)	Expected power produced in cell (W)	Excess power produced in cell (W)
		Rod 0.1 cm in diameter and 10 cm long			
25.13	2.84	0.0714	0.0402	0.0327	0.0075
	(2.49)	(0.0626)	(0.0314)	(0.0239)	
201.1	3.61	0.726	0.495	0.416	0.079
1608	9.67	15.55	13.73	13.07	0.654
	(8.13)	(13.07)	(11.25)	(10.60)	
		Rod 0.2 cm in diameter and 10 cm long			
50.27	2.70	0.136	0.094	0.058	0.036
402.1	4.21	1.696	1.57	1.074	0.493
3217	8.25	26.5	24.6	21.59	3.02
	(8.54)	(27.5)	(25.5)	(22.52)	
		Rod 0.4 cm in diameter and 10 cm long			
100.53	2.91	0.293	0.291	0.138	0.153
804.2	4.84	3.89	4.40	2.654	1.751
6434	8.60	55.3	72.2	45.4	26.8

ments were made by two methods. In initial experiments the current density was changed, and the power applied through a calibration resistor was adjusted to maintain a constant cell temperature (Table 2). For comparison, the reported excess specific power production for a Pd rod 0.20 cm in diameter (*1*) implies that an excess power of 0.14 W would be expected for our specimen at a current density of 64 mA/cm^2, whereas an excess specific power of 10 W/cm^3 would correspond to an excess power of 0.91 W for our sample. In later experiments the resistor power was stepped at constant electrolysis current density, and the resulting plot of the total applied power versus temperature was used to determine the heating power from the electrolysis circuit.

Several runs with the first method showed changes in the cell temperature that did not correspond to adjustments in the applied currents or voltages. These changes were clearly caused by changes in the heat transfer from the cells, rather than by some additional heating mechanism, because recalibration showed that the input electrolytic heating power was equal to the calculated enthalpy-corrected electrolysis power (P_{cell} with $\kappa = 1.0$) both before and after the temperature changes. The temperature changes typically were slow increases (often starting about 20 hours after the start of charging), and more rapid decreases, which occurred either spontaneously or occasionally after the addition of D_2O or H_2O. Without recalibration of the cell, such temperature increases could have been interpreted in terms of increased power production, but they actually reflected decreases in the rate of heat loss from the cell to the surroundings.

To differentiate further between an increase in output power and a change in rate of heat transfer, we measured the heating coefficient (the ratio of the temperature rise to the input heating power) of the Pd electrolysis cell by holding the electrolysis current density constant and incrementing the power applied through the calibration resistor. Figure 3 shows the dependence of the cell temperature upon the total applied heating power for a 0.1*M* $LiOH/H_2O$ cell, on the assumption that heating is the result of the sum of the calibration resistor power and the enthalpy-corrected electrolysis power (P_{cell} with $\kappa = 1.0$) of the Pd/Pt circuit. At a particular Pd/Pt electrolysis current density, the temperature at the location of the thermocouple was linearly dependent on the total input heating power over the temperature range 25° to 40°C, with a slope equal to the heating coefficient of the cell. Initially the heating coefficient decreased with increasing current density, consistent with additional heat losses caused by gas evolution, but 23 hours after the start of charging in the cell with a rod 3.9 mm in diameter the temperature increased. If the temperature rise had been due to an additional source of heat, the new heating line would have been parallel to the initial line, but displaced upward. Instead, the subsequent points defined a steeper line, indicating that the heating coefficient changed from 12° to 14°C per watt. Analysis of the data on cell temperature versus time indicated that the actual heating power produced by the electrolytic circuit remained constant to within 6%. Changes in heat transfer during bubble evolution in open systems have been reported (*6, 7*), and it is possible that a similar effect is occurring in the present system; in addition, changes in the volume of liquid owing to gas evolution and evaporation can also contribute to a time-dependent change in the heating coefficient of the cell (*8*), as could changes in the thermal conductivity of the cell walls or the electrodes (*9*). Moreover, at higher operating temperatures of the Dewar flask, nonlinearity in the relation of temperature to heating power of the calorimeter can lead to substantial overestimates of the electrolysis heating power, as can improper positioning of the temperature-sensing element relative to the resistive heater (*10, 11*). Clearly, accurate calorimetric measurements in this type of open cell require efficient stirring of the solution to eliminate temperature gradients, quantitative collection of the gases evolved, and calibration measurements at all electrolysis current densities and after all temperature changes; otherwise, it is not possible to unambiguously assign a rise in cell temperature to an increase in power production by the electrolysis circuit.

In conclusion, analysis of the data reported earlier (*1*) shows that the observed power production is much smaller than generally reported in the popular press and that several assumptions are required to transform the raw data into large excess power production ratios. In other recent experiments for which researchers have claimed excess power production in $Pd/D_2O/Pt$ electrolysis cells time-dependent changes have been observed in the slopes of electrolysis power versus tem-

Table 2. Representative calorimetry data for H_2O and D_2O electrolysis cells. The total power was calculated as the resistor power plus the electrolysis power. The measured temperatures are ±0.04°C; bath temperature = 27.000° ± 0.005°C. The error bars quoted were based on 2σ values for random errors in the multimeters and temperature measurement devices. The comparison between H_2O and D_2O gives an estimate of the magnitude of any systematic errors in the calorimeter.

Time (hours)	Current density (mA/cm^2)	Electrolysis power (W)	Resistor power (W)	Total power (W)	Temperature (°C)
		Drawn and machined Pd rod (0.21 to 0.22 by 2.1 cm), 0.1M LiOH/H_2O			
34.5	59	0.174 ± 0.002*	0.118 ± 0.001	0.292 ± 0.003	42.62
46.5	86	0.292 ± 0.003*	0	0.292 ± 0.003	42.68
67.5	59	0.175 ± 0.002*	0.119 ± 0.001	0.294 ± 0.003	39.82
77.5	86	0.297 ± 0.003*	0	0.297 ± 0.003	39.92
		Drawn Pd rod (0.22 by 2.4 cm), 0.1M LiOD/D_2O			
44.0	66	0.253 ± 0.003†	0.250 ± 0.002	0.502 ± 0.005	49.36
46.0	97	0.457 ± 0.003†	0.044	0.501 ± 0.003	49.39
72.0	97	0.473 ± 0.003†	0	0.473 ± 0.003	45.99
90.0	66	0.277 ± 0.003†	0.204 ± 0.002	0.481 ± 0.005	46.01

*Electrolysis power = $(E - 1.48\ V)\ I$. †Electrolysis power = $(E - 1.54\ V)\ I$.

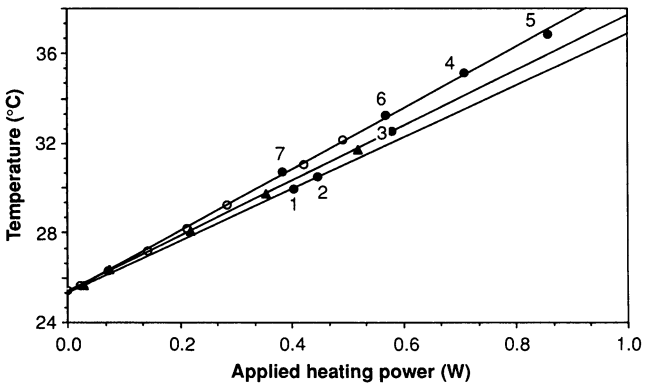

Fig. 3. Plot of the observed temperature versus the applied heating power for a Pd/H rod 3.9 mm in diameter and 2.4 cm long in 0.1*M* $LiOH/H_2O$, on the assumption that there is no recombination of evolved gases [that is, heating power = $I(E - 1.48\ V) + P_{resistor}$]. First, the calibration resistor was stepped in power with no electrolysis (○). Then current was applied at 8 mA/cm^2 for 17.1 hours, during which time the calibration resistor power was again stepped (▲). The electrolysis current was then increased to 60 mA/cm^2 for the remainder of the experiment (●). The labeled points were obtained at the following times after the second current step: 1, 3.6 hours; 2, 5.8 hours; 3, 8.7 hours; 4, 17.0 hours; 5, 21.2 hours; 6, 26.1 hours; 7, 30.4 hours. After 12 hours at 60 mA/cm^2, 0.7 cm^3 of H_2O was added to the cell (total cell volume = 30 cm^3).

perature plots (*12*), as opposed to changes in the intercepts of such plots. These data are consistent with a change in the heat loss constant (Fig. 3), as opposed to an increase in the rate of power production by the electrolysis cell. Careful calibration of the rate of heat loss and accounting for all sources of additional heat generation (gas recombination and so forth) are required before one can unambiguously assign a change in temperature of the electrolysis cell to an unexplained chemical or nuclear power–producing process. If required, more accurate power production measurements on the $Pd/D_2O/Pt$ system could only readily be made in closed-system calorimeters, where a well-defined heat path can be established and total recombination of the gases can be assured.

Note added in proof: In recent experiments in a closed-system calorimeter with total recombination of the gases, a recast Pd rod (0.39 cm in diameter and 1.0 cm in length) at 58 mA/cm^2 current density in 0.1*M* $LiOD/D_2O$ produced no measurable excess power [P_{meas} = (100 ± 2%) of P_{app}] for a period of over 12 days.

REFERENCES AND NOTES

1. M. Fleischmann, S. Pons, M. Hawkins, *J. Electroanal. Chem.* **261**, 301 (1989).
2. S. Gross, *Energy Convers.* **9**, 55 (1969).
3. A similar calculation has been independently performed: G. Kreysa, G. Marx, W. Plieth, *J. Electroanal. Chem.* **266**, 437 (1989). There are two errors in column c in table 2 of (*1*). The values for the rods of 0.2- and 0.4-cm diameter at 8 mA/cm^2 should be 143 and 306%, respectively.
4. J. M. Sherfey and A. Brenner, *J. Electrochem. Soc.* **105**, 665 (1958).
5. M. J. Joncich and N. Hackerman, *J. Phys. Chem.* **57**, 674 (1953).
6. R. G. Edkie and P. L. Khare, *Int. J. Heat Mass Transfer* **15**, 261 (1972).
7. S. C. Bhand *et al.*, *ibid.* **8**, 111 (1965).
8. W. E. Meyerhof, D. L. Huestis, D. C. Lorents, in preparation.
9. A. W. Szafranski and B. Baranowski, *J. Phys. E* **8**, 823 (1975).
10. R. Garwin, *Nature* **338**, 616 (1989).
11. N. S. Lewis *et al.*, paper presented at the Workshop on Cold Fusion Phenomena, 24 May 1989, Santa Fe, NM.
12. R. A. Huggins, *ibid.*

13. Supported by the Office of Naval Research and under a special grant from the California Institute of Technology. We thank G. Kreysa and W. Meyerhof for supplying preprints of related work. We thank C. A. Barnes and S. E. Kellogg for helpful criticism of this manuscript. Contribution 7969 from the Division of Chemistry and Chemical Engineering at the California Institute of Technology.

21 June 1989; accepted 29 August 1989

Dynamic Pore-Pressure Fluctuations in Rapidly Shearing Granular Materials

RICHARD M. IVERSON AND RICHARD G. LAHUSEN

Results from two types of experiments show that intergranular pore pressures fluctuated dynamically during rapid, steady shear deformation of water-saturated granular materials. During some fluctuations, the pore water locally supported all normal and shear stresses, while grain-contact stresses transiently fell to zero. Fluctuations also propagated outward from the shear zone; this process modifies grain-contact stresses in adjacent areas and potentially instigates shear-zone growth.

CLOSELY PACKED GRANULAR SOLIDS with interstitial pore spaces filled by liquid occur in both natural and man-made environments. Familiar examples include water-saturated soil and fragmented rock that compose most landslides, debris avalanches, and debris flows. Other examples include industrial slurries and granular mixtures, as well as saturated sediments that may be sheared during tectonic faulting.

Observations of mass-movement processes on the earth's surface have motivated fundamental questions about the dynamic role of pore water in rapidly sheared granular materials. For example, how can a water-saturated mass of landslide debris liquefy and flow tens of kilometers across slopes as gentle as a few degrees—much farther than similar masses of dry debris and much farther than anticipated from the material's initial potential energy and coefficient of internal friction (*1*)? In most theories, liquefaction caused by high, quasi-static pore-water pressure gradients has been invoked to account for the mobility of wet rock debris (*2*), but high pore-pressure gradients are unlikely to persist in debris that flows steadily for minutes or even hours. Furthermore, water is an ineffective lubricant on most rock surfaces (*3*). Thus, pore water must enhance efficient, rapid shear deformation of rocky debris by some alternative means.

In this paper we describe experiments testing a new hypothesis: that dynamic pore-pressure fluctuations can be generated as a result of grain rearrangements during rapid shear, and that the fluctuations can be large enough to modify grain-contact stresses significantly and promote efficient deformation. Specifically, transient increases in pore pressure in discrete domains where the granular phase momentarily contracts would inhibit further contraction and ease local shear displacement. Conversely, where the granular phase dilates, transient reduction in pore pressure would suppress further dilation and inhibit local shear displacement. In a deformation field in which local dilations and contractions accompany global shear, pore-pressure fluctuations may reduce frictional energy dissipation because they help localize intergranular shearing in areas of low or zero grain-contact stress (*4*). Such effects are enhanced if the pore fluid (for example, water) is relatively incompressible. An important lemma is that local dilation and contraction can occur even while the bulk deformation is steady (*5, 6*).

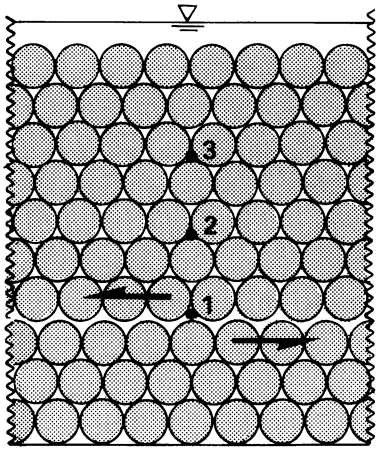

Fig. 1. Cross-sectional view through the center of the array of fiberglass rods. Water pressures were measured in individual pores indicated by numbered dots. Arrows show relative motion along the prescribed slip surface.

The tendency for pore-pressure fluctuations to develop during steady shear deformation depends on the relative rates of grain rearrangement and pore-pressure equilibration, which can be expressed by a single dimensionless parameter, $R = kE/\nu\mu\delta$ (*7, 8*) where k is the hydraulic permeability, E is the uniaxial (Young's) compression modulus of the composite granular medium, ν is the velocity of intergranular sliding, μ is the viscosity of the pore fluid, and δ is a characteristic length, typically the grain diameter. Within R the quantity kE/μ functions as a pore-pressure diffusivity, and $\delta^2\mu/kE$ is the time scale for diffusive pore-pressure equilibration over the distance δ. The quantity δ/ν is the time scale for pore dilation and contraction and thus for generation of pore-

U.S. Geological Survey, Cascades Volcano Observatory, 5400 MacArthur Boulevard, Vancouver, WA 97661.